Supplementary Data:

ANU Argon Facility Technical Report: ANU13-2020 & ANU14-2020
40Ar/39Ar Analysis for National Argon Map
By Marnie Forster and Davood Vasegh

NAM Proposals 02, 03 and 04:

- **Dating of mineralisation-related alteration in the Olympic Cu-Au Province, Gawler Craton**
- **Dating of mineralisation-related alteration at the Cairn Hill Mine, and regional thermal history of the northern Mt Woods Region, Gawler Craton**
- **Reconnaissance thermochronology of Curnamona Province**

Methods and procedures

Sample selection and mineral separation:

The samples in this study were provided by Geological Survey of South Australia and the separation procedures were undertaken in rock crushing and mineral separation laboratories at The Australian National University (Table 1). No chemical or leaching treatments were used during separation.

Mineral separation begins by choosing the most pristine sections with no evidence of weathering or staining. For samples with a targeted microstructure, the rock is first sliced into thin slabs using a trim saw, the selected area was then cut from the rock using a band saw. Once the selected area was separated, it was then crushed, milled and de-slimed as many times as was necessary to clean the grains and finally washed in deionised water.

K-feldspar procedure:

For these minerals the grains are sieved into size fractions: 250-420μm and passed through 0.25A then 1.0A current using a Frantz magnetic separator. K-feldspars are concentrated in the non-magnetic 1A fraction. This grain fraction is then separated under gravity using the Lithium heteropolytungstates (aq) (LST) heavy liquid at 2.58 g/cm3. K-feldspars are concentrated in the lighter than 2.58 g/cm3 size fraction. The separated grains are washed as many times as was necessary to remove any residue LST on the grains with deionised water. Final hand-picking of the best quality grains was done in the Argon Preparation Laboratory.

White Mica (Muscovite) procedure:

For these minerals the grains are sieved into size fractions: 250-420μm, based on actual grain size in the sample. Additional white mica is obtained through 0.25A then 1.0A current using a Frantz magnetic separator. Final hand-picking of the best quality grains was done in the Argon Preparation Laboratory.
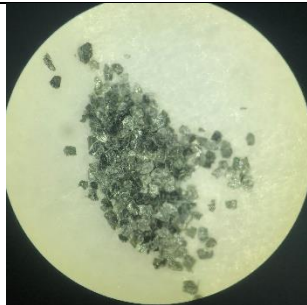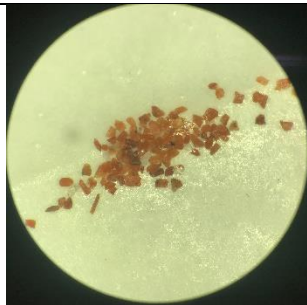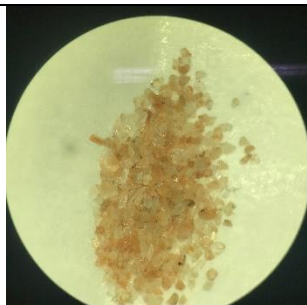
Biotite (Phlogopite) procedure:

For these minerals the grains are sieved into size fractions: 250-420μm, based on actual grain size in the sample. Paper concentration is performed on the 250-420 μm size fraction to obtain the purest mineral separation as possible. Additional biotite is obtained by separating grains through 0.25A current using a Frantz magnetic separator, with biotite concentrated in the magnetic 0.25A fraction. Final hand-picking of the best quality grains was done in the Argon Preparation Laboratory.
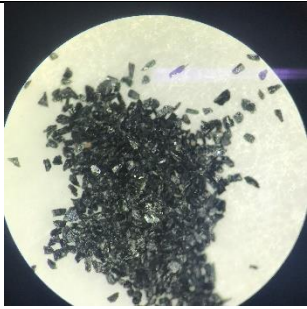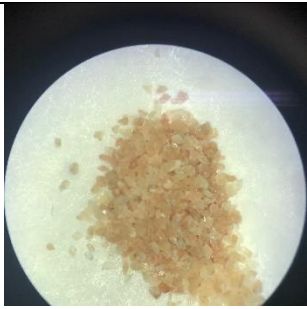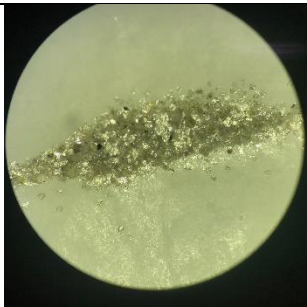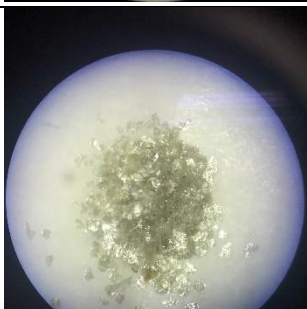
Hornblende procedure:

For these minerals the grains are sieved into size fractions: 250-420μm based on actual grain size. Grains in the 250-420 μm size fraction is selected and passed through 0.25A current using a Frantz magnetic separator. Hornblendes are concentrated in the magnetic 0.25A fraction. If the separates from FRANTZ are not pure (i.e. ≥ 50% hornblende), this grain fraction is then separated under gravity using the Lithium heteropolytungstates (aq) (LST) heavy liquid at 2.9 g/cm3.

Hornblendes are concentrated in the heavier than 2.9 g/cm3 size fraction. The separated grains are washed as many times as was necessary to remove any residue LST on the grains with deionized water Final hand-picking of the best quality grains was done in the Argon Preparation Laboratory.

Mineral separation details:

Sample ID	Target Mineral	Mass (mg)	Grain Size (µm)	Treatment / Comment	Picture
2131356	Muscovite	3.2	420-250	Chloritised mica crystals with green-black hue	
2111462	K-feldspar	4.4	420-250	Dark orange K-feldspar crystals, pure fraction	
2131370	Biotite	4.9	420-250	Shiny black biotite crystals, pure fraction	
2131370	K-feldspar	3.3	420-250	White and orange K-feldspar crystals with rare tiny dark inclusions, clean fraction.	
1998157	Phlogopite	4.3	420-250	Dark black phlogopite aggregates with dull sheen.	

1978579	Hornblende	30.8	420-250	Clean prismatic hornblende crystals, pure fraction	
1978579	K-feldspar	3.8	420-250	Creamy white-orange K-feldspar crystals, pure fraction	
2016096	Muscovite	3.1	420-250	Shiny white-mica crystals with rare dark inclusions, clean fraction	
2016096	Biotite	4.2	420-250	Shiny black biotite crystals in a mixture with some white-mica and quartz crystals	
2016087	Muscovite	2.6	420-250	Shiny white-mica crystals, pure fraction	
2016087	Biotite	4.8	420-250	Shiny black biotite crystals, pure fraction	

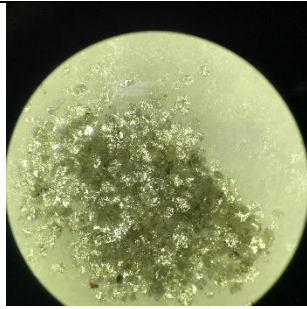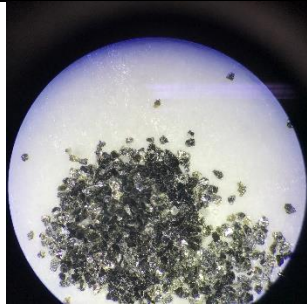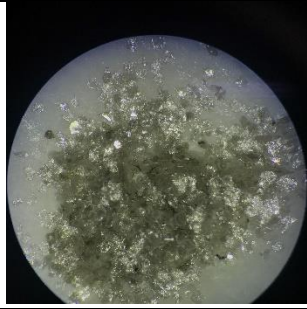|					
2016108	Muscovite	3.7	420-250	Shiny white-mica crystals, pure fraction	
2016108	Biotite	4.4	420-250	Shiny black biotite crystals, pure fraction	
1707876	Muscovite	3.2	420-250	Shiny white-mica crystals, pure fraction	
1707876	Biotite	4.7	420-250	Black-green chloritized biotite crystals, clean fraction	

Table 1: Mineral separation details

Sample irradiation details:

Irradiation of samples for $^{40}Ar/^{39}Ar$ analysis was undertaken at the University of California Davis McClellan Nuclear Research Centre, CA, US in Central Facility position of TRIGA reactor without rotation, with 1.0mm of Cadmium shielding as ANU CAN #36 for 12.08 hours on 11-12 August 2020. The calculated amounts of grains were weighed and recorded and then wrapped in labelled aluminium packets in preparation for irradiation. The sample filled foils were placed into a quartz irradiation canister together with aliquots of the flux monitor Biotite GA1550. The foil packets of GA1550 standards were dispersed 6-8mm apart throughout the irradiation canister, between the unknown age samples. In addition, packets containing K_2SO_4 and CaF_2 were placed in the middle of the canister to monitor argon isotope production from potassium and other interfering elements.

Irradiated samples were unwrapped upon their return to the Australian National University, and then rewrapped in tin foils in preparation for analysis under vacuum in the furnace. Tin foil is used because the melting temperature of tin is lower than the experiment starting point in the furnace and gasses from tin can be pumped away prior to the sample analysis.

$^{40}Ar/^{39}Ar$ procedures and analysis information

Methodology:

Temperature-controlled resistance furnace step-heating experiments is the technique that is used in the ANU Argon laboratory to extract argon isotopes from the samples to ensure 100% release of ^{39}Ar. A sample is dropped into a cleaned furnace and heated to 400°C to melt the tin foil and then left in the furnace at 350°C for 8-12 hours to pump away unwanted gases. This cleaning procedure has proven to significantly improve the quality of the resultant data. The step-heating experiment then starts at 450°C, and each incremental heating step is heated at a constant temperature for 15 minutes. The heating process involves rapid heating to the setpoint temperature with no overshoot, then temperature is maintained for 15 minutes followed by rapid cooling; this procedure produces a square wave in temperature for each heating step. The heating step schedule for biotite and muscovite rises by 30°C increments (except for the last a few steps), with 30 steps per sample, while K-feldspar is analysed in more than 40 steps, including numerous isothermal steps. Diffusion experiments, as conducted in the ANU Argon laboratory, are designed to retrieve diffusion parameters which can be used in quantitative temperature-time modelling. The heating schedules are recorded in the Excel Tables for each sample.

Cleaning of the furnace between samples is vital in this method. The furnace is degassed four times at 1,450°C for 15 minutes and the gas pumped away prior to the loading of the subsequent sample. Blanks are measured to monitor the cleaning process. The flux monitor crystals are fused using a CO_2 continuous-wave laser. Gas released from either the flux monitors or each step of the sample analyses are exposed to three Zr-Al getters; two AP10 (Cold and hot) and one CP50, each for 10 minutes, to remove active gases. The purified extracted gasses are then isotopically analysed in the Argus VI mass spectrometer. The $^{40}Ar/^{39}Ar$ dating technique is adapted from McDougall and Harrison (1999) and described in Forster and Lister (2009).

Background levels are measured and subtracted from all analyses, from flux monitors and samples. The nuclear interfering values for the correction factors for the isotopes are listed below (Tetley et al 1980). These are measured for the reactions and uncertainties of $(^{36}Ar/^{37}Ar)_{Ca}$, $(^{39}Ar/^{37}Ar)_{Ca}$, $(^{40}Ar/^{39}Ar)_K$, $(^{38}Ar/^{39}Ar)_K$ and $(^{38}Ar)_{Cl}/(^{39}Ar)_K$, and were calculated prior to sample analyses.

Mass spectrometer setup and procedures

Samples and standards were analysed in the Argon Laboratory at the Research School of Earth Science, The Australian National University, Canberra, Australia using a *Thermo Fisher ARGUS-VI* multi-collector mass spectrometer (Table 2).

Mass Spectrometer:	Thermo Fisher Argus VI
Detector Type:	Faraday Cups only x5
Calibrations:	3 levels (Zero Offset, Gain and Cross Calibration)
Peak Centring:	Once for every measurement @H2 (^{40}Ar)
Measurement Cycles:	51 cycles on all detectors
Extrapolation Method:	Exponential extrapolation and uncertainty

Name	UFC Offset [fA]	Gain	Cross Calibration Factor
H2	-4.9761469	0.9871203	1
H1	-2.2071069	0.9671459	1.007184188
AX	-7.6814703	0.9769602	1.017518151
L1	-2.3979322	0.9706487	1.030604297
L2	-3.1329948	0.9676338	1.047244337

Table 2: Detector Calibration Values

The calculation parameters:

Lambda ^{40}K (Renne et al 2011)	5.5305E-10
Lambda ^{37}Ar (Kondev et al 2017)	1.9798E-02
Lambda ^{39}Ar (Kondev et al 2017)	7.0548E-06
Lambda ^{36}Cl (Kondev et al 2017)	6.2985E-09
Flux Monitor	GA1550 @ 99.18 ± 0.14 Ma
Total irradiation power	12.08 MW
Irradiation Date	11-12 Aug, 2020
Irradiation shielding	Cadmium 1.0mm

Interfering isotope production ratios:

$(^{36}Ar/^{37}Ar)_{Ca}$ correction factor	1.01283E-04
$(^{39}Ar/^{37}Ar)_{Ca}$ correction factor	8.46943E-03
$(^{40}Ar/^{39}Ar)_{K}$ correction factor	1.34009E-01
$(^{38}Ar/^{39}Ar)_{K}$ correction factor	1.05445E-02
$(^{38}Ar)_{Cl}/(^{39}Ar)_{K}$ correction factor	8.18472E-02
Ca/K conversion factor	1.90

Atmospheric Argon correction ratio:

$^{40}Ar/^{36}Ar$	(Lee et al 2006)	298.57
$^{40}Ar/^{38}Ar$	(Lee et al 2006)	1,583.52

Representative air shot and blanks measurements:

The discrimination factor was calculated by analysing five air shots on either side of sample analyses and is reported at 1amu. Table 3 shows an example of the analysed air shots and resultant calculation of discrimination factor.

Date	^{40}Ar ± %err		^{38}Ar ± %err		^{36}Ar ± %err		1amu ± %err		Reported Value
01-Dec-2020	1,851.556	0.015	1.379	2.326	6.313	0.567	1.00448	0.288	
01-Dec-2020	1,848.823	0.015	1.310	2.894	6.354	0.633	1.00648	0.321	1.0048686 ± 0.213%
01-Dec-2020	1,848.496	0.014	1.291	2.982	6.278	0.663	1.00349	0.336	
01-Dec-2020	1,845.605	0.013	1.372	2.566	6.276	0.691	1.00381	0.349	
01-Dec-2020	1,865.401	0.011	1.280	2.424	6.401	0.637	1.00608	0.323	

Table 3: Air Shots and Mass Discrimination Factor

The blank measurements are undertaken with different temperature schedules between 300°C and 1450°C, depending on the degassing behaviour and previous blank measurement results. The degassing and blank measurement procedure continues until the ratios of ^{40}Ar, ^{38}Ar and ^{36}Ar drop to atmospheric ratios, and ^{39}Ar and ^{37}Ar drop below detectable levels. The entire procedure of degassing and blank measurements is repeated at the end of a set of samples. Blanks will be done in-between samples that belong to a set, with reduced steps at 300°C, 1300°C and 1450°C to check isotope levels. In addition, the mass of each sample is calculated so that the volume of gas released from each step overwhelms the volume of gas that may occur in the blank. The table 4 is a representative sequence of measured blank values recorded during a monitoring process.

Temperature	^{40}Ar	^{39}Ar	^{38}Ar	^{37}Ar	^{36}Ar	$^{40}Ar/^{36}Ar$
300	1817.738	0.708661	1.209615	ND*	6.113996	297.3077
500	1879.391	0.741332	1.266375	ND	6.364901	295.2743

700	1911.306	0.759696	1.282523	0.095807	6.417252	297.8386
900	2053.27	0.775687	1.358664	ND	6.94095	295.8198
1100	2731.788	0.812587	1.788944	0.10454	9.192207	297.1852
1300	7305.089	1.038774	4.728446	0.139915	24.59727	296.9878
1450	36811.09	2.436249	23.78145	0.23653	124.4077	295.8909
300	748.5261	0.344558	0.467985	0.019884	2.5069	298.5864
1300	1126.281	0.438838	0.704102	0.0207706	3.744338	300.7958
1450	2181.428	1.00614	1.377076	0.1028531	7.299197	298.8587

Table 4: Example of the blanks measurements during a sequence of blanks where isotopes were being monitored prior to sample analysis (* => Not Detectable). Temperature is °C.

Data reduction software:

The calculations were done with an adapted version of *Noble* Software (2020, developed and adapted by the Australian National University Argon Laboratory) and all interpretations have been undertaken with *eArgon* (developed and adapted for ANU Argon Laboratory by G.S. Lister).

Reported Data:

The reported data have been corrected for system backgrounds, mass discrimination, fluence gradients and atmospheric contamination. GA1550 standards were analysed, and an exponential best fit was then used for the calculation of the J-factor and J-factor uncertainty (Table 5).

Samples J-Factor, Mass Discrimination, and uncertainties:

Sample Name	J-Factor ± %uncertainty		Mass Discrimination Factor ± %uncertainty		Measurement Date
2131356	2.18769E-03	0.2436	1.00485	0.142	13-Nov-2020
2111462	2.18596E-03	0.2436	1.00496	0.211	17-Nov-2020
2131370	2.18422E-03	0.2436	1.00496	0.211	22-Nov-2020
2131370	2.18248E-03	0.2436	1.00496	0.211	24-Nov-2020
1998157	2.18074E-03	0.2436	1.00487	0.213	27-Nov-2020
1978579	2.17901E-03	0.2436	1.00487	0.213	03-Dec-2020
1978579	2.17553E-03	0.2437	1.00499	0.142	05-Dec-2020
2016096	2.17380E-03	0.2437	1.00445	0.226	07-Dec-2020
2016096	2.17206E-03	0.2437	1.00445	0.226	10-Dec-2020
2016087	2.17032E-03	0.2437	1.00445	0.226	12-Dec-2020
2016087	2.16859E-03	0.2437	1.00430	0.197	15-Dec-2020
2016108	2.16685E-03	0.2437	1.00430	0.197	17-Dec-2020
2016108	2.16511E-03	0.2437	1.00403	0.103	19-Dec-2020
1707876	2.16338E-03	0.2437	1.00436	0.087	29-Dec-2020
1707876	2.16164E-03	0.2438	1.00436	0.087	30-Dec-2020

Table 5: Sample analysis and calculation details

^{40}Ar/^{39}Ar isotopic data of the samples are supplied in the Excel Data Tables, which include details on the heating schedule, Argon isotopes abundances and their uncertainty levels, %Ar*, ^{40}Ar*/^{39}Ar(K), Cumulative ^{39}Ar%, calculated age and its uncertainty, Ca/K, Cl/K, J-Factor and its uncertainty. Noting that all the reported uncertainties are at one sigma level and the fractional uncertainties are shown as % in the headings of the appropriate columns of data tables. The components involved in the calculation of the uncertainties are listed in Table 6.

Uncertainty of:	Components involved in the calculation
Isotope Abundances	Uncertainty of isotope measurement Uncertainty of Mass Discrimination Factor (except for ^{39}Ar)
J-Factor	Uncertainty of ^{40}K Decay Constant Uncertainty of Age of the Flux monitor Uncertainty of Flux monitor isotopes abundances
Calculated Age	Uncertainty of Isotopes Abundances J-Factor value and uncertainty of J-Factor ^{40}K Decay Constant value and uncertainty of ^{40}K Decay Constant

Table 6: Components involved in the calculation of each uncertainty

References:

Forster, M.A. and Lister, G.S. 2004. The interpretation of 40Ar/39Ar apparent age spectra produced by mixing: application of the method of asymptotes and limits. J*ournal of Structural Geology* **26,** 287–305

Forster, M.A. and Lister, G.S. 2009. Core-complex-related extension of the Aegean lithosphere initiated at the Eocene-Oligocene transition. *Journal Geophysical Research*, **114**, B02401.

McDougall, I. and Harrison, T.M. (Eds.). 1999. Geochronology and Thermochronology by the ^{40}Ar/^{39}Ar Method, 2nd ed., 269 pp. Oxford Univ. Press, New York.

Kondev, F.G. and Naimi, S. 2017. The NUBASE2016 evaluation of nuclear properties. *Chinese physics C*, **41**(3), p.030001.

Lee, J.Y., Marti, K., Severinghaus, J.P., Kawamura, K., Yoo, H.S., Lee, J.B. and Kim, J.S. 2006. A redetermination of the isotopic abundances of atmospheric Ar. *Geochimica et Cosmochimica Acta*, **70**(17), 4507-4512.

Renne, P.R., Mundil, R., Balco, G., Min, K., and Ludwig, K.R. 2010. Joint determination of 40K decay constants and 40Ar*/40K for the Fish Canyon sanidine standard, and improved accuracy for 40Ar/39Ar geochronology. *Geochemica et Cosmochimica Acta,* **18**, 5349–5367.

Tetley, N., McDougall, I. & Heydegger, H.R. 1980. Thermal neutron interferences in the ^{40}Ar/^{39}Ar dating technique. *Journal Geophysical Research*, **85**, 7201–7205.